HiSST: 3rd International Conference on
High-Speed Vehicle Science Technology
14 -19 April 2024, Busan, Korea

Temperature Effect on Erosion by Atomic Oxygen in LEO Environment Using Reax-FF Molecular dynamics

Jiwon Jung[1], Jongkyung An[2], Seunghwan Kwon[3], Gun Jin Yun[4]

Abstract

While operating spacecraft in Leo Earth Orbit (LEO), polymers are damaged by extreme environments in space. Especially, highly reactive oxygen atoms are continuously bombarded on the surface, leading to polymer erosion. In this study, atomic oxygen (AO) bombardment simulation on Kapton using Reax-FF molecular dynamics (MD) was undertaken to calculate erosion yield at the LEO-operating temperature regime and quantify temperature dependency. Unlike previous studies under NVE ensemble, the convergence of erosion yield after saturation of AO on the system was observed, and from the Arrhenius plot of the erosion yield, the phase transition effect was also found by relatively long-time NVT simulations.

Keywords: Atomic oxygen, molecular dynamics, Reax-FF, Low earth orbit, polymer aging

1. Introduction

Spacecraft operating in LEO (altitudes between 200km and 700km) encounter hazardous environments which damage structural materials. The main hazards in LEO were reported as 1) high-reactivity atomic oxygen (AO), which erodes surfaces; 2) UV radiation, which is energetic enough to break polymer bonds; and 3) extreme thermal change in high vacuum. [1] Among these environments, the bombardment of AOs on the polymer surface leads to the oxidation of the surface and generation of volatile gas molecules. The polymer mass loss by AO erosion makes the material properties to be degraded and may cause severe breakdown in satellite systems. Therefore, the Materials International Space Station Experiment 2 (MISSE2) project was designed to study the effects of extreme space environments by affixing materials to the exterior of the ISS for prolonged exposure. Through MISSE2 project, the researchers were allowed to study materials degradation mechanisms, structural changes, and performance characteristics over time [2]. Nevertheless, owing to the high cost and limited availability of such in-flight experiments, it cannot be conducted as many as desired.

Thus, ground simulations and computational methods have been studied to describe extreme environments in LEO. Since construction of experimental equipment for ground simulations is also expensive to facilitate high vacuum, severe UV, thermal control at least from 200K to 400K, and cosmic plasma. Therefore, computational methods including molecular dynamics (MD) methods had been many researchers to predict the effect of AO on a polymer surface and explore materials to protect satellites from AOs. In the fields of MD, the Reax-FF has been mainly adopted for AO bombardment simulations. While dynamics of atoms in MD are determined by their interactions defined by the interatomic force fields, conventional MD force fields relies on fixed bonds and they never change during

[1] *Aerospace Engineering Department, Seoul National University, 1, Gwanak-ro, Gwanak-gu, Seoul, Republic of Korea, zwjohn94@snu.ac.kr*
[2] *Aerospace Engineering Department, Seoul National University, 1, Gwanak-ro, Gwanak-gu, Seoul, Republic of Korea, ajk7419@snu.ac.kr*
[3] *Aerospace Engineering Department, Seoul National University, 1, Gwanak-ro, Gwanak-gu, Seoul, Republic of Korea, sh.kwon@snu.ac.kr*
[4] *Aerospace Engineering Department, Seoul National University, 1, Gwanak-ro, Gwanak-gu, Seoul, Republic of Korea, gunjin.yun@snu.ac.kr*

the simulations without any additional modification for formation of new bonds and dissociation of existing bonds. Meanwhile, the Reax-FF developed by Adri C. T. van Duin and William A. Goddard III can update bonds between atoms by calculating bond orders during simulations [3]. Therefore, the Reax-FF had been utilized for describing molecular events including chemical reactions such as combustion, oxidation, AO bombardments, etc.

In 2014, Rahnamoun and Van Duin presented the first attempt to mimic AO bombardment in LEO. They compared the mass loss from AO erosion and temperature evolution of Teflon, polyhedral oligomeric silsesquioxane (POSS)-Kapton, Kapton, and silica. [4]. Rahmani et al. compared AO erosion resistance between Kapton, POSS-grafted Kapton, graphene or CNT–Kapton nanocomposites systems [5].Ashraf et al. conducted AO bombardment simulations on epoxy systems, exploring different combinations of resin and hardener molecules. They qualitatively demonstrated the effects of crosslink percentage and temperatures [6].Park et al. studied AO erosion in SiC structures with different surface orientations as a thermal protection system and reported on the oxidation transition observed during the simulations. [7]. Jeon et al. presented comparison between AO and nitrogen bombardment effects on Kapton, POSS-grafted Kapton, graphene or CNT-Kapton nanocomposites [8].

Nevertheless, since MD simulations were conducted under time steps with femtosecond units, there are huge time scale discrepancies to experimental scales. Especially, in previous MD AO bombardment simulations, which were mainly conducted under the NVE (constant particles, volume, energy) ensemble to depict adiabatic conditions, the temperature rises to over 1000K to 1500K within several picoseconds. Therefore, qualitative comparisons of AO resistance were mainly conducted. However, in LEO, the surface temperature of spacecraft varies from 200K to 400K, so molecular simulations at such temperature and quantification of temperature effect on erosion yield are necessary. Although several studies conducted Reax-FF simulations with the NVT ensemble at LEO temperatures, there were no significant discussions beyond mentioning tendencies of increasing erosion yield in high-temperature conditions. Thus, in this study, we conducted AO bombardment simulations to Kapton, to quantify erosion yield at LEO-operating temperature regime and temperature effects using Reax-FF MD.

2. Methods

2.1. Molecular model

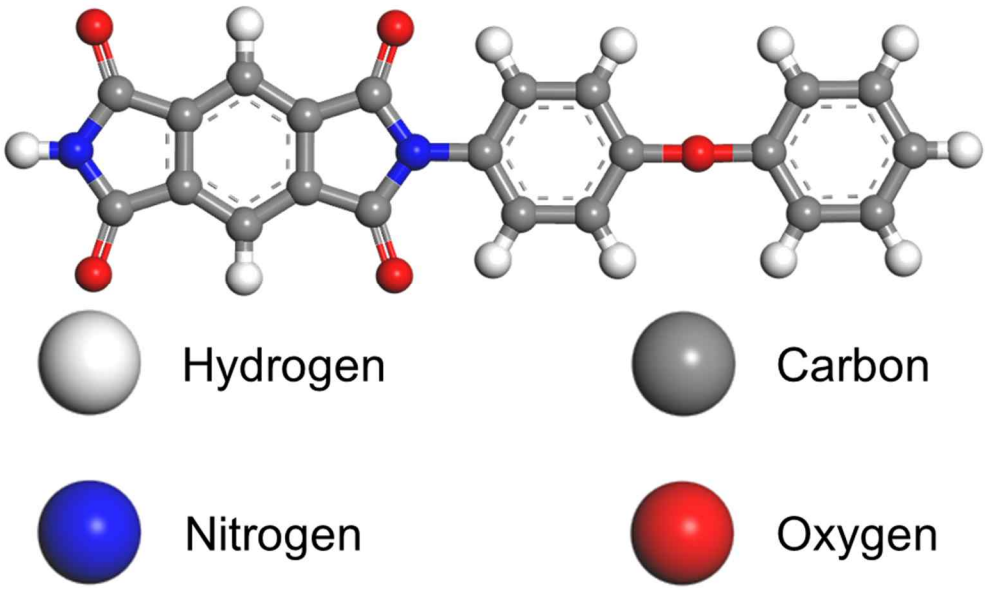

Fig 1. Representation of the Kapton monomer

In our simulation, the Polyimide(Kapton) was studied, which is a light-weight, thermally stable, UV-resisting and great insulation material. Thanks to such characteristics, Kapton has been applied as a space coating materials to protect surface of the satellite structures. The Kapton monomer is shown in

오류! 참조 원본을 찾을 수 없습니다., where ten repeat units were polymerized in a single chain. The whole molecular model consists of 4 Kapton chains, of which 40 Kapton monomers (1568 atoms) were included. The initial amorphous cell model of the Kapton were built by the commercial molecular dynamics software, Materials Studio [9].

For the AO bombardment simulation, to shoot AOs on the Kapton surface are necessary, the 2D polymer slab without periodic boundary to z direction should be built and located on the bottom of the simulation. Since initial cell were constructed on the periodic boundary conditions on each x,y,z directions, untangling polymer entanglements through z direction and formation of the slab are required. Following the scheme proposed in previous works, the molecular model was largely tensioned to desired direction and then annealed on high temperature to make polymer clump into a slab. In high temperature, thermodynamic activity at the stretched state induce entanglements between chains to be resolved and van der waals interaction makes them to be attract each other. The initial cubic model was stretched to total strain of 400% through 1,000,000 time steps then relaxed by 1,000,000 steps of NVT ensemble at 600K. The modification process of the model into the slab are illustrated in Fig.2.

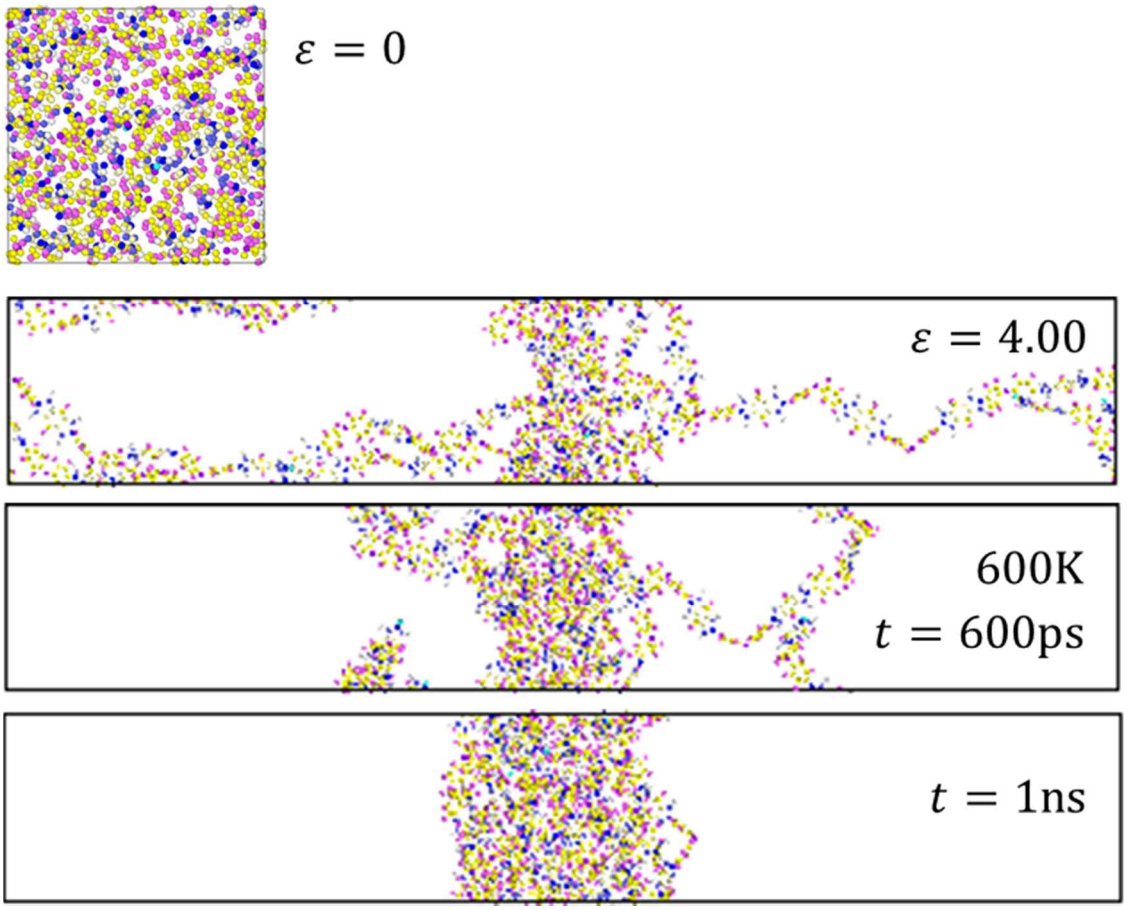

Fig 2. Modeling of the Kapton slab from the amourphous Kapton

In the generation of the slab model, the all-atom force field of polymer consistent force field(PCFF) [10] was used. The position of the slab was then translated into the bottom of the cell, and height was modified to 100Å. The cross-sectional area of the model had a size of $27.2\text{Å} \times 27.2\text{Å}$, where periodic boundary conditions were applied to x and y directions. At the 4Å from bottom of the slab were fixed its atom coordinates, and oxygen atoms were discharged from the top of the simulation box, with 7.4km/s velocity, which is an orbital speed in LEO (altitude ~400km) every 200fs toward –z direction. The AO bombardment simulations were conducted with time steps of 0.1fs, for 200ps, where total 1000 oxygen atoms were discharged. Each AO atoms had about 5eV of kinetic energies to interact on the surface of Kapton. The NVT simulations were conducted for every 40K from 200K to 800K after 100,000 relaxation steps at each temperature. At each temperature, simulations were conducted 5 times and averaged for their results. Volatile molecules generated after the AO bombardment were deleted when they reached the top of the simulation box to prevent molecules to interact on the surface multiple

times, and depict vacuum environment of LEO. During molecular dynamics simulations, Nose-Hoover thermostat was applied to control temperature [11]. The overall description of the simulation cell is represented at Fig. 3.

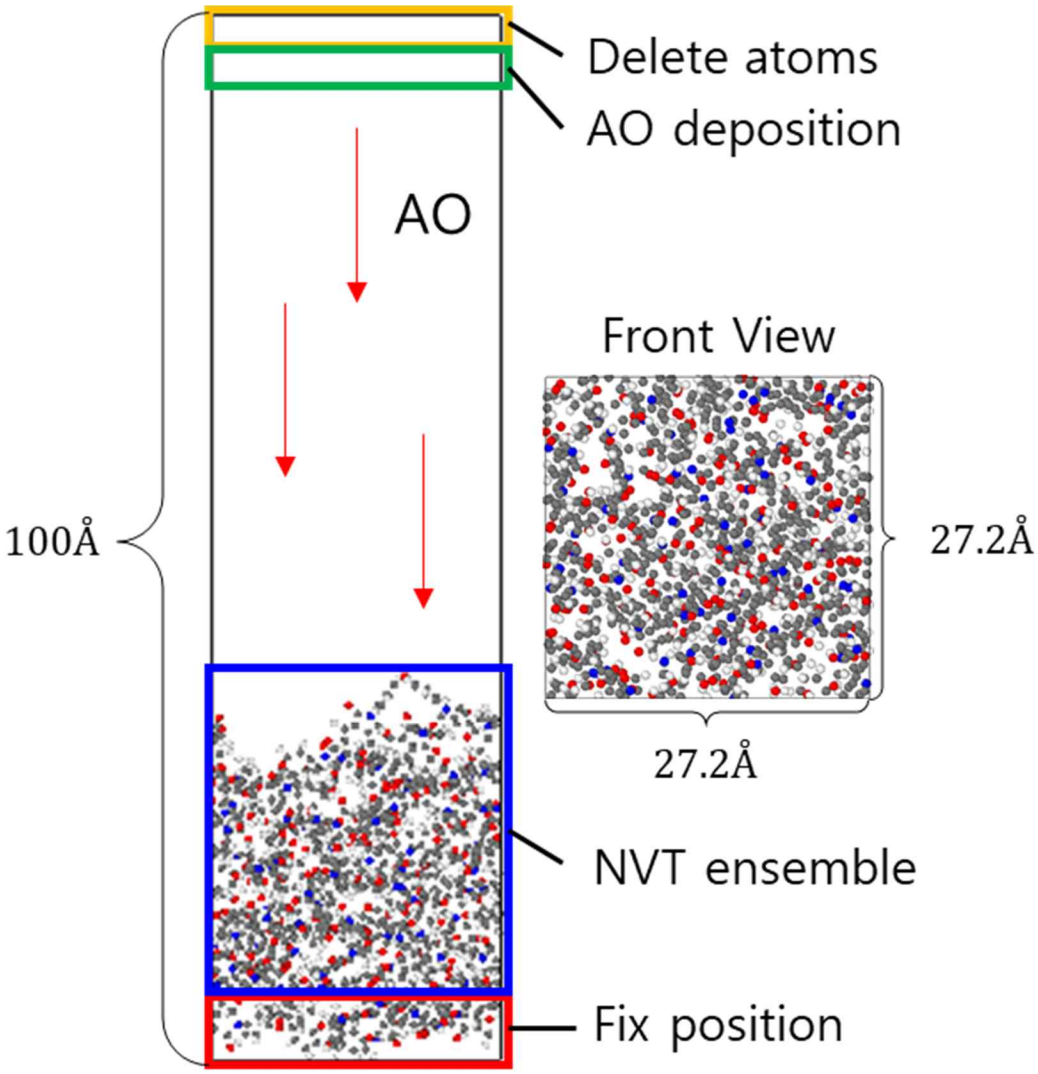

Fig 3. Molecular dynamics AO bombardment simulation cell description

2.2. Reax-FF

In classical all-atom MD force fields such as PCFF, they have fixed bonds and they are maintained until the end of the simulation unless additional commands to manipulate chemical bonds. Therefore, chemical reactions are not able to be captured from the classic force fields. However, The Reax-FF developed by the Adri Van-Duin group can actively depict the formation and dissociation of chemical bonds by updating bond orders from interatomic distances with relatively small computational efforts compared to first-principle-based calculations [3]. Thanks to such advantages, Reax-FF has been popular in studying chemical reactions in the nanoscale, including combustion, AO bombardment and oxidation. In Reax-FF, the total energy of each atom is calculated as Eq. (1), where E_{bond} = bond energy, E_{over} = over coordination energy, E_{under} = under coordination energy, E_{lp} = lone pair energy, E_{val} = valence energy, E_{tor} = torsional energy, $E_{vdW\ aals}$ = Van der Waals energy, $E_{Coulomb}$ = Coulomb energy, and E_{rest} = restrain energy. Interatomic bond orders are defined as Eq. (2), a summation of bond orders from σ, π, and π-π from the left.

$$E_{system} = E_{bond} + E_{over} + E_{under} + E_{lp} + E_{val} + E_{tor} + E_{vdW\ aals} + E_{Coulomb} + E_{rest} \quad (1)$$

$$BO_{ij} = BO_{ij}^{\sigma} + BO_{ij}^{\pi} + BO_{ij}^{\pi-\pi} \quad (2)$$

From the original version of the Reax-FF for hydrocarbons, the Reax-FF had been developed and expanded for various elements by additional training data sets derived from the DFT calculation and experiments. The Reax-FF used in this study was adopted from AO bombardment simulation on POSS-Kapton and Teflon, developed by Rahnamoun et al. [4], which includes reactive interatomic potentials between silicon, carbon, oxygen, hydrogen and nitrogen atoms.

2.3. Optimization of the time step

Since the selection of the time steps in Reax-FF not only affects atomic movements, but also the reactivity of molecules, it might critically influence simulations in AO bombardment and gas generation. In previous studies of AO bombardment on several different materials, time steps of 0.25fs and 0.1fs were used for different studies. Therefore, the effects of time steps were investigated for NVE simulations using time steps of 0.25fs, 0.1fs, and 0.05fs. Other conditions, such as total simulation times, time intervals between AO depositions, initial cell configuration, and AO velocities, were identical for each simulation. As AOs were deposited every 200fs, they were launched from the top of the cell every 800, 2000, and 4000 time steps for each simulation, respectively. The entire simulations were conducted for a duration of 100 AO atom depositions, resulting in a total analysis time of 20ps. As represented in Fig. 4, a drastic increase in temperature was observed after 10ps in the 0.25fs time step condition compared to the 0.1fs and 0.05fs conditions. On the contrary, there was no significant difference in temperature evolution between the 0.1fs and 0.05fs conditions.

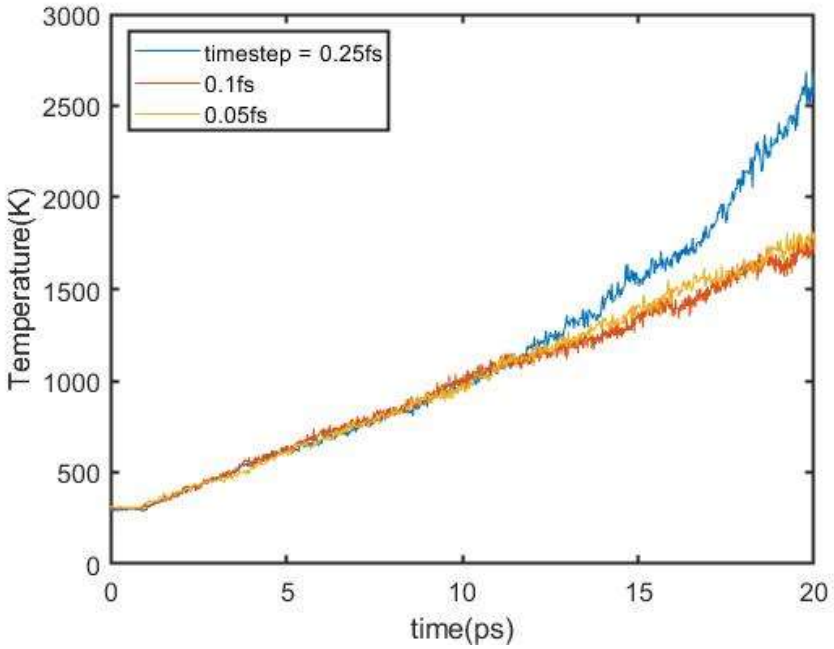

Fig 4. Temperature evolution during NVE simulation of AO bombardment on Kapton

Such discrepancy in temperature evolution in simulations can be interpreted as a difference in the formation of chemical energy from bond breakage and the formation of volatile molecules by AO bombardments. As presented in Fig. 5, a sharp rise in the mass loss rate of the slab after 10ps was observed in the 0.25 fs condition, implying a greater generation of gaseous molecules. Therefore, it leads to the release of additional energy from surface chemical bonds into the simulation cell. A larger time step allows atoms with the same velocities to move a larger distance in a single time step, making it feasible for atoms to move beyond the bond order distance of Reax-FF. Therefore, overestimation of the erosion yield by AO was induced by the larger time steps. Simulations with smaller time steps can provide more accuracy; however, they require more computational resources. Proper selection of the time step is necessary. Therefore, a time step of 0.1fs was selected for our following analysis, as there was no relevant distinction between results from 0.1fs and 0.05fs simulations.

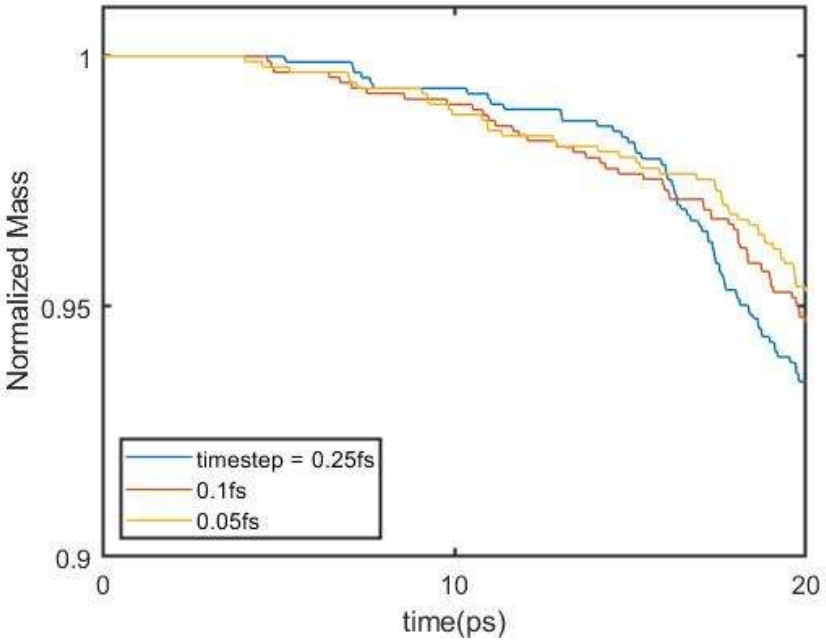

Fig 5. Normalized mass change of the Kapton slab for different time steps

3. Results

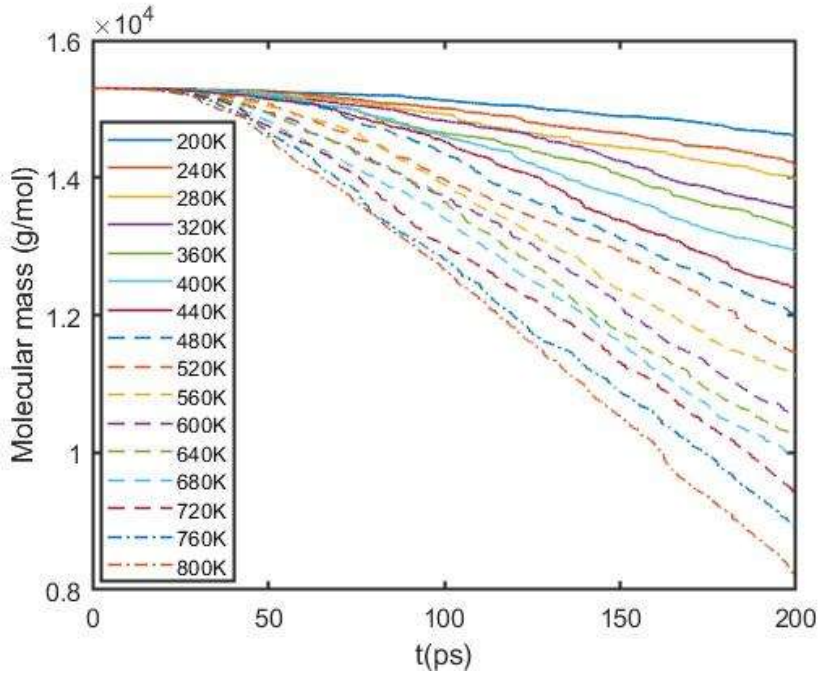

Fig 6. Mass loss during the NVT simulations

The mass change during the AO bombardments in each temperature condition is plotted at Fig. 6. As revealed from previous qualitative studies on the temperature effect on AO erosion, the results showed an accelerated erosion rate in high-temperature conditions. As shown in the plot, at the onset of the bombardments, the remaining molecular mass of the slabs changes nonlinearly. However, after 100ps, 500AOs were discharged, the remaining mass changed linearly, and the erosion rate converged. In previous studies, bombardment analyses were conducted with relatively few AOs, typically 50 to 100, and erosion yield was calculated from the nonlinear part of the mass curves. The overall curve during AO bombardment can be divided into such change in mass loss pattern. At the first stage of bombardments, AOs were accumulated at the surface of the polymer. Therefore, the mass loss of the

slabs were smaller than the latter stage. After the polymer surface was oxidized enough and oxygen atoms were saturated, the polymer started to degrade at a consistent rate.

Furthermore, the saturation of oxygen in polymer surface and linearization of the mass loss occurred faster in high temperature conditions. Whereas the mass of the Kapton slab started to decrease linearly from 50 ps of simulation time (250 AOs), the polymer started to erode linearly around 75 ps (375 AOs) and 100 ps (500 AOs) for the 480K and 200K conditions, respectively. Such tendencies can be more clearly illustrated by the presence of volatile gas molecules in the simulation box, as shown in Fig. 7. Hydrogen oxide molecules such as OH and H_2O are generated from the early stage of the simulation, and their populations were sustained until the end of the simulation, even though they were deleted when they reached the top of the box, throughout the entire simulation. Meanwhile, carbon oxide molecules were not actively generated in the first stage of the simulations, but the gas production rate sharply increased at a certain point. Since hydrogens do not consist polymer backbone structures, they can easily dropped from the surface and form volatile species with oxygens from bombardments. On the other hand, as carbon atoms are backbones of Kapton, the production rate of CO atoms indicates the degradation of the structure of the polymer. Therefore, they hardly found in the simulation box at the first stage of the bombardments. Following the patterns in mass changes, rapid growth of CO molecule generation occurred at higher temperatures, as illustrated in Fig. 7(a). At higher temperatures, the polymer surface atoms have more thermodynamic energy to react with approaching oxygen atoms, making them more likely to be oxidized than in low-temperature conditions. Therefore, less simulation times and AOs were needed to be saturated.

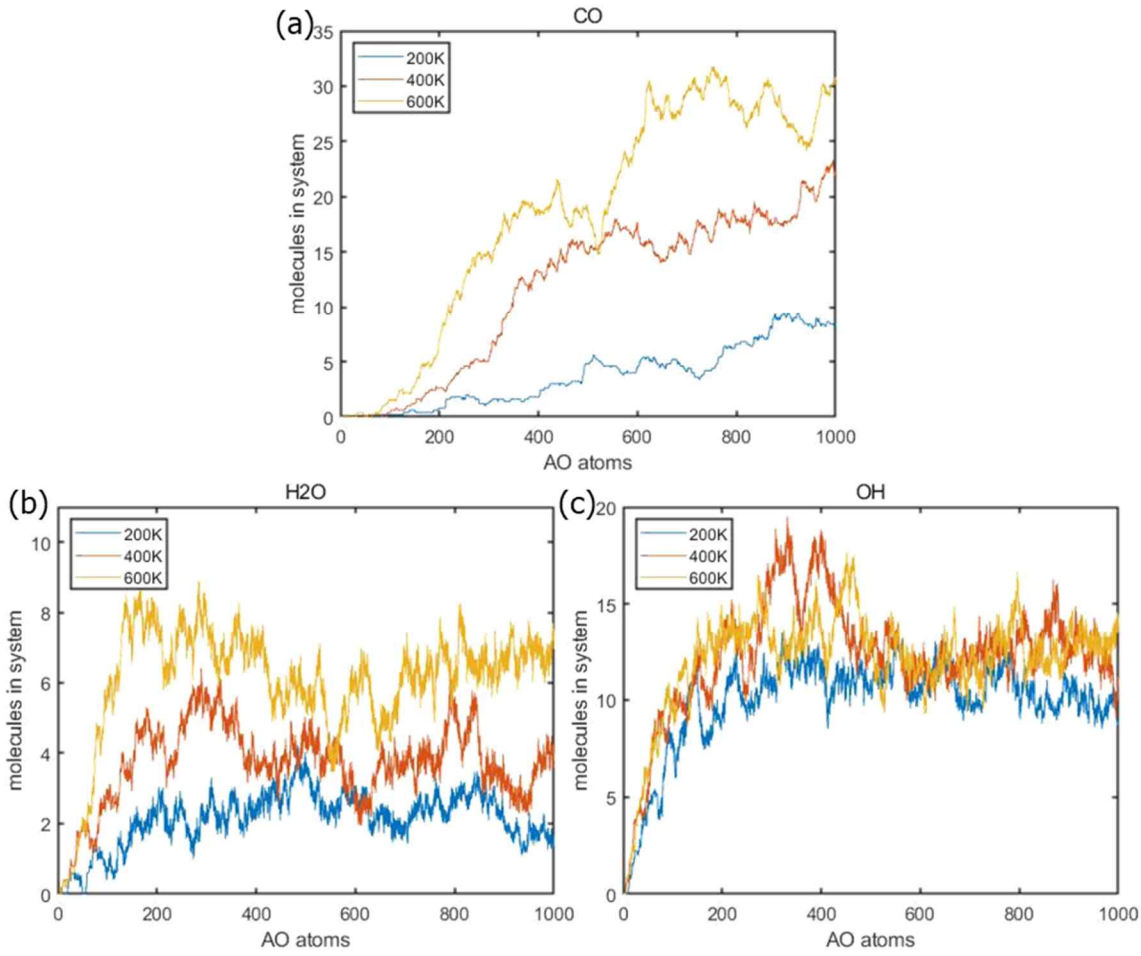

Fig 7. Number of (a) CO, (b) H_2O, and (c) OH molecules existing in simulation cells at different temperatures

To quantify the temperature dependency of the AO erosion rate, the Arrhenius plot was plotted in Fig. 8. As represented in the figure, the overall shape of the figure can be fitted as a bilinear curve. In the low-temperature regime, the logarithm of the erosion yield showed a linear relationship with the reciprocal of the temperature, and then the slope of the curve increased after certain temperature point.

The erosion phase transition temperature of the Kapton was determined from the intersection point of the linearly fitted lines from the high-temperature erosion curve and the low-temperature erosion curve. Therefore, the transition temperature was found to be 630K, which falls within the range of the glass transition temperature of Kapton (360°C ~ 410°C) determined from experiments [11].

The erosion yield as a function of temperature is expressed on Eq. (3), two linear curves in different temperature ranges divided by the glass transition temperature where $\dot{m}$ is the erosion yield having unit of g/AO, T is the absolute temperature, E_a is the activation energy for AO erosion reaction, A is the Arrhenius factor, and k_B is the Boltzmann coefficient. The parameters in the equation are listed on Table 1.

$$\dot{m} = Ae^{-\frac{E_a}{k_B T}} \tag{3}$$

Table 1. Parameter values for the characterization of temperature effect on AO erosion

A (g/AO)	E_a(J)	(T_g = 630K)
1.87 X 10^{-23}	6.53 X 10^{-21}	$T<T_g$
9.69 X 10^{-23}	2.08 X 10^{-20}	$T>T_g$

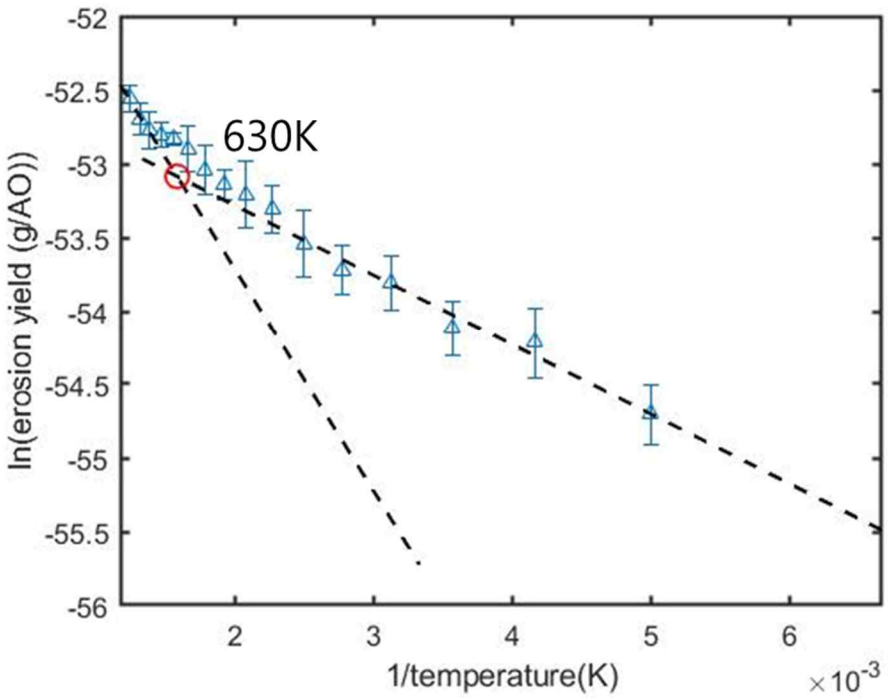

Fig 8. Arrhenius plot of the erosion yield and prediction of the phase transition

The prediction of the glass temperature point by the Arrhenius plot of the erosion yield implies that the phase transition of a polymer to the rubbery state can accelerate oxidation and erosion by AOs. When the polymer was in the rubbery state, as oxygen atoms were likely to diffuse through polymer chain networks, they can easily make bonds with backbone carbon atoms, rather than remaining on the surface of the polymer. Moreover, after forming bonds with backbone atoms, since they can move more dynamically than in glassy state, volatile gas molecules were easier to be separated from the bulk material. Furthermore, in the operating temperature regime in LEO (200K~400K), the results showed yield values of $2 \times 10^{-24} g/AO \sim 6 \times 10^{-24} g/AO$, which more closely matched to the experimentally observed yield of Kapton [2], than previous molecular simulations [4, 8].

4. Conclusion

This paper presented AO bombardment simulations with Reax-FF in LEO-operating temperature using long-time NVT ensembles for Kapton. In previous NVE simulations, the temperature of the simulation box rose over 2000K in the tens of picoseconds. Therefore, it was not proper to match with erosion yield from experimental results directly, but to compare AO resistance between materials qualitatively. At the initial stage of the bombardment, AOs were accumulated on the surface oxidized the polymer surface. Therefore the slab mass was degraded nonlinearly and hydrogen oxide products such as OH and H_2O were mainly generated. After oxygen atoms were saturated, the slab mass started to decrease linearly and carbon oxide molecules such as CO were produced from the main backbone atoms of the polymer. Such mass degradation pattern change occurs in early time steps in high temperature conditions that oxidation probabilities were higher by more thermodynamic energy of surface. Furthermore, while mapping the Arrhenius plot of the erosion yield, the overall curve was fitted into the bilinear curve and the glass transition temperature of Kapton was predicted by the intersection point of two fitted lines. Moreover, even though there is still a discrepancy in time scales with experimental scales, erosion yield was highly matched to experimental results in operating temperature in LEO.

Acknowledgment

This research was financially supported by the Institute of Civil-Military Technology Cooperation, funded by the Defense Acquisition Program Administration and the Ministry of Trade, Industry, and Energy of the Korean government under grant No. 22-CM-19. The authors are grateful for the support.

References

1. Grossman, E. and I. Gouzman: Space environment effects on polymers in low earth orbit. Nuclear Instruments and Methods in Physics Research Section B: Beam Interactions with Materials and Atoms. 208, 48-57 (2003)
2. De Groh, Kim K., et al.: MISSE 2 PEACE polymers atomic oxygen erosion experiment on the international space station. High Performance Polymers 20(4-5), 388-409 (2008)
3. Van Duin, A. C. T., et al.: ReaxFF: A Reactive Force Field for Hydrocarbons. Journal of Physical Chemistry A. 105(41) 9396-9409 (2001)
4. Rahnamoun, A. and A.C. van Duin: Reactive molecular dynamics simulation on the disintegration of Kapton, POSS polyimide, amorphous silica, and teflon during atomic oxygen impact using the ReaxFF reactive force-field method. Journal of Physical Chemistry A. 118(15), 2780-7 (2014)
5. Rahmani, Farzin, et al.:Reactive molecular simulation of the damage mitigation efficacy of POSS-, graphene-, and carbon nanotube-loaded polyimide coatings exposed to atomic oxygen bombardment. ACS Applied Materials & Interfaces 9(14), 12802-12811. (2017)
6. Ashraf, C., et al.: Reactive Molecular Dynamics Simulations of the Atomic Oxygen Impact on Epoxies with Different Chemistries. The Journal of Physical Chemistry C. 123(24), 15145-15156 (2019)
7. Park, T., et al.: Investigation of Silicon Carbide Oxidation Mechanism Using ReaxFF Molecular Dynamics Simulation. Journal of Spacecraft and Rockets. 57(6), 1328-1334 (2020)
8. Jeon, I., S. Lee, and S. Yang: Hyperthermal erosion of thermal protection nanocomposites under atomic oxygen and N2 bombardment. International Journal of Mechanical Sciences. 240, 107910 (2023)
9. BIOVIA, Dassault Systèmes, Materials Studio 2017 R2, San Diego: Dassault Systèmes, (2017).
10. Sun, H., et al.: An ab initio CFF93 all-atom force field for polycarbonates. Journal of the American Chemical society. 116(7), 2978-2987 (1994)
11. Evans, Denis J., and Brad Lee Holian.: The nose–hoover thermostat. The Journal of chemical physics 83(8), 4069-4074 (1985)
12. DuPont, D.: KAPTON® summary of properties. EI-10142 (1/22), (2022)